Distinct Immune Reconstitution Profiles Captured by Immune Functional Assays at 6 Months Post Allogeneic Hematopoietic Stem Cell Transplantation

William Mouton, Anne Conrad, Vincent Alcazer, Mathilde Boccard, Maxime Bodinier, Guy Oriol, Fabien Subtil, Hélène Labussière-Wallet, Sophie Ducastelle-Lepretre, Fiorenza Barraco, et al.

Transplantation and Cellular Therapy 29 (2023) 94.e1–94.e13

Transplantation and Cellular Therapy

journal homepage: www.tctjournal.org

ASTCT American Society for Transplantation and Cellular Therapy

Full Length Article
Biology

Distinct Immune Reconstitution Profiles Captured by Immune Functional Assays at 6 Months Post Allogeneic Hematopoietic Stem Cell Transplantation

William Mouton[1,2,a], Anne Conrad[3,4,5,a], Vincent Alcazer[6,7], Mathilde Boccard[1,3,4], Maxime Bodinier[1], Guy Oriol[1], Fabien Subtil[8,9], Hélène Labussière-Wallet[6], Sophie Ducastelle-Lepretre[6], Fiorenza Barraco[6], Marie Balsat[6], Gaëlle Fossard[6], Karen Brengel-Pesce[1], Florence Ader[3,4,5,*], Sophie Trouillet-Assant[1,2]

[1] *Joint Research Unit Hospices Civils de Lyon-bioMérieux, Hospices Civils de Lyon, Lyon Sud Hospital, Pierre-Bénite, France*
[2] *Virology and Human Pathology - Virpath Team, International Centre for Research in Infectiology (CIRI), Claude Bernard Lyon 1 University, Lyon, France*
[3] *Legionella Pathogenesis Team, International Centre for Research in Infectiology (CIRI), Claude Bernard Lyon 1 University, Lyon, France*
[4] *Infectious and Tropical Diseases Department, Hospices Civils de Lyon, Croix-Rousse Hospital, Lyon, France*
[5] *Claude Bernard Lyon I University, Villeurbanne, France*
[6] *Clinical Hematology Department, Hospices Civils de Lyon, Lyon Sud Hospital, Pierre-Bénite, France*
[7] *LIB TEAM, International Centre for Research in Infectiology (CIRI), Oullins, France*
[8] *Biostatistics Department, Hospices Civils de Lyon, Lyon France, Lyon 1 University, Villeurbanne, France*
[9] *CNRS, Biometrics and Evolutionary Biology Laboratory UMR, Villeurbanne, France*

Article history:
Received 20 July 2022
Accepted 27 October 2022

Key Words:
Hematopoietic stem cell transplantation
Allogeneic
Immune functional assay
Gene expression
Herpesviridae reactivation

A B S T R A C T

Immune reconstitution after allogeneic-hematopoietic-stem-cell transplantation (allo-HSCT) is a complex and individual process. In this cross-sectional study, whole-blood (WB) immune functional assay (IFA) was used to characterize immune function by assessing immune-related gene/pathway alterations. The usefulness of this tool in the context of infection, 6 months after transplantation, was evaluated. Sixty allo-HSCT recipients at 6 months after transplantation and 10 healthy volunteers (HV) were included. WB was stimulated in standardized TruCulture tubes using lipopolysaccharides and *Staphylococcal* enterotoxin B. Gene expression was quantified using a custom 144-gene panel using NanoString nCounter technology and analyzed using Ingenuity Pathway Analysis. The relationships between immune function and clinical characteristics, immune cell counts, and post-transplantation infections were assessed. Allo-HSCT recipients were able to activate similar networks of the innate and adaptive immune response compared to HV, with, nevertheless, a lower intensity. A reduced number and a lower expression of genes associated with immunoregulatory and inflammatory processes were observed in allo-HSCT recipients. The use of immunosuppressive treatments was associated with a protracted immune reconstitution revealed by transcriptomic immunoprofiling. No difference in immune cell counts was observed among patients receiving or not receiving immunosuppressive treatments using a large immunophenotyping panel. Moreover, the expression of a set of genes, including *CCL3/CCL4*, was significantly lower in patients with *Herpesviridae* reactivation (32%, 19/60), which once again was not identified using classical immune cell counts. Transcriptional IFA revealed the heterogeneity among allo-HSCT recipients with a reduced immune function, a result that could not be captured by circulating immune cell counts. This highlights the potential added value of this tool for the personalized care of immunocompromised patients.

Allogeneic hematopoietic stem cell transplantation (allo-HSCT) is a cellular therapy aiming at curing malignant and non-malignant hematological diseases or primary immunodeficiencies [1,2]. From an immunological point of view, allo-HSCT recipients are a complex and heterogeneous population who undergo a state of complete immunosuppression followed by an individual and gradual immune reconstitution. This dynamic process is routinely monitored by cell count measurements, mainly through $TCD4^+$ and $TCD8^+$ cell counts in clinical settings [3–8]. Several underlying conditions and post-transplantation complications such as graft-versus-host disease (GvHD) and associated

*Correspondence and reprint requests: Florence Ader, Département des Maladies Infectieuses et Tropicales, Hôpital de la Croix-Rousse, Hospices Civils de Lyon, 103 Grande-Rue de la Croix-Rousse, 69317, Lyon cedex 04, France.
E-mail address: florence.ader@chu-lyon.fr (F. Ader).
[a] W.M. and A.C. are co-first authors.

https://doi.org/10.1016/j.jtct.2022.10.025

immunosuppressive treatments can impact immune reconstitution and lead to immune deficiency and/or dysregulation. Protracted immune reconstitution is associated with an increased infectious risk that represents a major cause of morbidity and mortality [9–14].

A recent study found a 23.8% mortality rate related to infections, from a wide spectrum of infectious agents which can be specific to the post-transplant period [15]. The spectrum of infections after allo-HSCT appears to be related to the kinetics of immune reconstitution notably during the late phase post-engraftment where a close relationship is suggested between infections and the recovery of immune function [12]. In case of deficient or altered immune system, the reactivation of latent viruses mainly belonging to the *Herpesviridae* family (cytomegalovirus [CMV], human herpesvirus-6 [HHV-6], or Epstein-Barr virus [EBV]) may result in symptomatic infections that can lead to fatal complications [16–18].

In the post-transplantation time-course, a better comprehension of the relationship between immune cell function and the occurrence of infections would thus be essential. Despite the routine use of traditional biological markers, only limited information is available regarding the functionality of immune cells. Indeed, immune reconstitution is mainly monitored through static readouts such as quantitative cell counts or soluble/surface marker measurements that do not reflect functional alterations. An assessment using reproducible and standardized tools is thus needed [19–25].

The contribution of whole-blood immune functional assays (IFA) to characterize immune functionality has been assessed in healthy volunteers (HV) [26] and in septic patients [27]. To date, a single study has investigated pre- and post-allo-HSCT cytokine responses [28]. We intended to further describe the functionality of innate and adaptive immune cells using whole-blood IFA, combining transcriptomic and proteomic readouts. In this proof-of-concept study, we took advantage of the initiation of the vaccination schedule at 6 months after transplantation to differentially characterize the immune reconstitution of allo-HSCT recipients in comparison with HV.

The immune response of allo-HSCT recipients was hypothesized to be different than that of HV. This hypothesis led to 2 objectives: first, to get further insights of the heterogeneity of immune reconstitution, and second to assess immune profiles according to clinical characteristics and transplantation-related events, including GvHD. For that purpose, we used standardized whole-blood stimulation assays (TruCulture; Rules Based Medicine, Austin, TX) after stimulation by lipopolysaccharides (LPS), a toll-like receptor-4 and -2 ligand, which triggers the innate immunity [29,30], or *Staphylococcal* enterotoxin B (SEB), a superantigen binding simultaneously the major histocompatibility complex class II and the T cell receptor, initiating the adaptive response [31,32]. TruCulture has been described as a reliable monitoring tool, which enables the classification of inflammatory and host immune responses by evaluating the variance in poststimulation immune responses between healthy donors and patients [27,28].

MATERIALS AND METHODS

Study Population

Sixty adult (≥18 years old) allo-HSCT recipients who underwent transplantation at the hematology department of the Lyon University Hospital (France) were included in the prospective, single-center cohort study "VaccHemInf" between May 2018 and August 2020 [33] at 6 months after transplantation (interquartile interval [IQR], 5-8 months), before the initiation of the recommended vaccination schedule [34]. The exclusion criteria applied were post-transplantation relapse of the hematological underlying disease or death [33].

The cohort was approved by the regional ethics committee (Comité de Protection des Personnes Sud-Est V, Grenoble, France, number 69HCL17_0769) and is registered in ClinicalTrials.gov (NCT03659773). At inclusion, demographics (age, sex), hematological and transplantation-related characteristics (underlying disease, conditioning regimen, stem cell source, donor type), as well as post-transplantation characteristics (GvHD, immunosuppressive treatment, post-transplantation infections) were retrieved from medical records through an electronic case report form. All infectious episodes occurring either 14 days before or 14 days after blood sampling were retained, and no specific additional microbiological investigation was performed for the study. Regarding reactivations of *Herpesviridae*, whole-blood CMV and EBV DNA-emia was monitored at least weekly up to 100 days after transplantation, then monthly during the first year after transplantation, and on demand (as for HHV-6) in case of clinical symptoms compatible with viral disease. In the absence of consensual cutoff values for viral DNA-emia, viral reactivations were deemed significant and recorded in case of attributable symptoms or based on the viral load in the absence of symptoms (≥3 log copies IU/mL for CMV once or more, ≥3 log copies IU/mL for EBV twice or more, ≥4 log copies IU/mL for HHV-6 twice or more). CMV DNA-emia ≥3 log copies IU/mL prompted pre-emptive treatment, whereas EBV and HHV-6 reactivations were handled according to the rate of increase of EBV copy number or the presence of HHV-6 related clinical symptoms [35–38].

Concomitantly, 10 HV were recruited among donors at the Lyon Blood Bank Center (Etablissement Français du Sang) and were evaluated as a control group. According to the Etablissement Français du Sang standardized procedures for blood donation and the provisions of article R.1243–49, and following one of the French public health codes, a written non-opposition to the use of donated blood for research purposes was obtained from the HV. The personal data from the blood donors were anonymized before being transferred to our research laboratory. Regulatory authorizations for the handling and conservation of these samples were obtained from the regional ethics committee (Comité de Protection des Personnes Sud-Est II) and the French ministry of research (Ministère de l'Enseignement supérieur, de la Recherche et de l'Innovation, DC-2008–64).

Post-transplantation T-cell Immunophenotyping

Extensive immunophenotyping by flow cytometry on whole blood was performed at the immunology laboratory of the Lyon university hospital. Counts of white blood cells, polynuclear neutrophils, monocytes, natural killer cells, total T-cell, naive $CD4^+$ and $CD8^+$ ($CD45RA^+CCR7^+$) T cells, central memory ($CD45RA^-CCR7^+$) $CD4^+$ and $CD8^+$ T cells, effector memory ($CD45RA^-CCR7^-$) $CD4^+$ and $CD8^+$ T-cells, differentiated memory $CD4^+$ and $CD8^+$ T-cells ($CD45RA^+CCR7^-$) were determined (cells/μL) as previously described [33].

Immune Functional Assays: Truculture Stimulation

Blood from patients and HV was drawn on site, and heparinized whole-blood (1 mL) was subsequently distributed within 1.5 hours (±30 minutes) after sampling into prewarmed, standardized, ready-to-use tubes (TruCulture) containing the medium alone (NUL) or the medium with LPS (100 ng/mL) or the medium with SEB (400 ng/mL). As previously described, tubes were then inserted into a dry block incubator and maintained at 37°C for 24 hours [26]. After incubation, cellular pellets were harvested and re-suspended in 2 mL TRI Reagent LS (Sigma-Aldrich Corp., St. Louis, MO), vortexed for 2 minutes, and rested for 10 minutes at room temperature before storage at −80°C.

RNA Extraction

For TruCulture cell pellet handling and RNA processing and detection, the protocol was carried out according to the study by Urrutia et al. [39]. Cell pellets from TruCulture stimulations kept in TRI Reagent LS (Sigma-Aldrich) were thawed under agitation. Before processing, thawed samples were spun in a centrifuge (3000*g* for 5 minutes at 4°C) to pellet cellular debris generated during the Trizol lysis. For extraction, a modified protocol of the NucleoSpin 96 RNA tissue kit (Macherey-Nagel) was followed using a vacuum system. Briefly, 600 μL of clarified Trizol lysate was transferred to a tube preloaded with 900 μL of 100% ethanol. The mixture was transferred into the columns, washed with buffers MW1 and MW2 (×2) and RNA was eluted using 30 μl RNase-free water. Aliquots for gene expression analysis were prepared and frozen at -80°C until use. RNA concentration was estimated using the Nanodrop One spectrophotometer (Thermo Scientific, Swedesboro, NJ) according to the process provided by the manufacturer.

Gene Expression Analysis

The NanoString nCounter technology [40], a hybridization-based multiplex assay characterized by its amplification-free step, was used for mRNA detection of a 144-gene panel (Supplementary Table S1, online) designed with genes from a previous publication [39] and genes known to be crucial in the immune response. According to manufacturer's instructions, 300 ng of

RNA were hybridized to the probes at 67°C for 18 hours using a thermocycler. After removal of excessive probes, samples were loaded into the nCounter Prep Station (NanoString Technologies, Seattle, WA) for purification and immobilization onto the internal surface of a sample cartridge for 2 to 3 hours. The sample cartridge was then transferred and imaged on the nCounter Digital Analyzer (NanoString Technologies) where color codes were counted and tabulated for the 144 genes. Data treatment and normalization were next performed using nSolver analysis software (version 4.0, NanoString technologies). Each sample was analyzed in a separate multiplexed reaction, each including 8 negative probes and 6 serial concentrations of positive control probes.

Negative control analysis was performed to determine the background for each sample. A first step of normalization using the internal positive controls allowed correction of a potential source of variation associated with the technical platform.

To do so, we calculated for all samples the background level as the median +3 standard deviations across the 6 negative probe counts (obtained threshold: 30). Every sample under the background level was fixed to this value. Next, we calculated for each sample the geometric mean of the positive probe counts. A scaling factor for a sample was a ratio of the geometric mean of the sample and the average across all geometric means. For each sample, we divided all gene counts by the corresponding scaling factor. To normalize for differences in RNA input we used the same method as in the positive control normalization, except that geometric means were calculated over 3 housekeeping genes (DECR1 (NM_001359.1), HPRT1 (NM_000194.1) and POLR2A (NM_000937.2). The 3 housekeeping genes were selected using NormFinder, GeNorm, BestKeeper, and DeltaCT methods; an established approach for the identification of stable housekeeping genes within and between groups, from the 6 candidate genes included in the custom panel [41–44].

Gene Expression Interpretation

After normalization steps, the ratio between stimulated condition (either LPS or SEB) and the control condition (NUL) were calculated to compare gene expression levels between allo-HSCT recipients and HV. Results were expressed as fold change (FC) induction. Differentially-expressed genes (DEG) after stimulation were defined as a gene expression with a minimum of 2FC (up or down) between the 2 conditions (NUL versus LPS or SEB). Of note, for this analysis, the 3 housekeeping genes were removed from the panel, as well as genes with a raw count below the background noise threshold (30 counts) in more than 75% of individuals (n = 3 and n=7, after SEB and after LPS, respectively).

Biological network enrichment was performed using the "core analysis" function of the Ingenuity Pathway Analysis software (IPA, QIAGEN) by adding the list of DEG [False discovery rate FDR (adjusted $P < .05$ and FC > 2), with identifiers and corresponding expression values (FC). The Fisher's exact test P value was used as a readout for the assessment of biological network activation. The different algorithms used have been previously described [45,46]. Activation score for each biological networks was calculated as previously described [47]; for details please refer to the supplementary methods.

Protein Detection

Interleukin (IL)-6, IL10, CXCL10 and interferon gamma (IFN-γ) protein from healthy volunteers and allo-HSCT recipients in TruCulture supernatant was quantified on Simple/Multi-plex cartridges (ProteinSimple, San Jose, CA) using ELLA nanofluidic system (Biotechne, Minneapolis, MN), according to the manufacturers' instructions. Results are expressed in pg/mL.

Statistical Analysis

Normality testing was performed using the Shapiro-Wilk normality test. Distribution of quantitative data was expressed as mean (range) or median (interquartile range, IQR) where appropriate. For HV and allo-HSCT recipient datasets, analysis of variance was performed using F-tests, and differences were calculated using a parametric unpaired Student's t test with Welch's correction. Gaussian data were analyzed using analysis of variance and non-gaussian data using the Kruskal-Wallis test or the Mann-Whitney test, when appropriate. Area under receiver operating characteristic (ROC) curves (AUC [95% confidence interval {95%CI}]) and volcano/whisker plots were plotted using GraphPad Prism software (version 8; GraphPad software, La Jolla, CA). ROC curves were built to identify the most differentially expressed genes between patients with or without viral infectious episodes.

Principal component analysis (PCA) and hierarchical clustering was carried out using Partek Genomics Suite software (version 7.0; Partek Inc., St. Louis, MO). The analysis according to the administration of immunosuppressive treatments was conducted using Linear Discriminant Analysis applied on the 5 first component of the PCA to get 80% of the explained variability using "adegenet" R package [48]. The impact on gene expression of clinical characteristics known to determine speed and quality of immune reconstitution (age, sex, underlying disease, parameters of T-cell reconstitution, parameters of allo-HSCT procedure, GvHD, ongoing immunosuppressive treatment) was analyzed using Wilcoxon test [3,49]. Heatmap was generated by scaling and centering log10-transformed gene expressions, and the dendogram was drawn based on hierarchical clustering analysis (Euclidean distance matrix with Ward's method). Statistical analyses were conducted using R (version 3.6.2.). P values and adjusted P values (P adj) $< .05$ were considered significant.

RESULTS

Participant Characteristics

Overall, 60 patients who underwent allo-HSCT were included at a median (IQR) time of 6 (5-8) months after transplantation. Acute myeloid leukemia was the most common underlying disease (52%, n = 31). Before inclusion, manifestations of acute and chronic GvHD (aGvHD and cGvHD) were reported in 70% (n = 42) and 13% (n = 8) of allo-HSCT recipients, respectively. At the time of inclusion, 27% (n = 16) of patients had not experience any GvHD, 38% (n = 23) had a resolved GvHD, and 35% (n = 21) still presented an active GvHD, independently of the form (acute or chronic). A total of 32% (n = 19) of recipients were on immunosuppressive therapy (Table 1). Concomitantly, 10 HV were included, matched for age (median [IQR]: 49.0 [33.5-56] versus 44.5 [34-60] years for allo-HSCT; $P = .98$) and sex (sex ratio, 0.7 versus 1.3 for allo-HSCT, $P = .50$).

Allo-HSCT Recipients and HV are able to Activate Similar Biological Networks on SEB and LPS Whole-Blood Stimulation

First, an unsupervised analysis of the full gene-panel transcriptomic data using PCA showed a robust space aggregation of each experimental condition (i.e., NUL, SEB, and LPS stimulation) in both populations with an explained variance of 81.6% and 68.0% for HV and allo-HSCT recipients, respectively (Figure 1A,B). Combining the HV and allo-HSCT populations, the variance was mainly explained by stimulation (PC1 46.7%) and by the stimulant-related effect (PC2 14.8%; Figure 1C). Next, in both populations, the activation of biological networks represented by the top 5 activated canonical pathways, upstream regulators, and disease and functions upon SEB (Figure 1D) and LPS (Figure 1E) stimulation was assessed. Among the 15 biological networks described, 11 were induced both by LPS and SEB stimulation, among which 4 canonical pathways, 3 upstream regulators and 4 diseases and functions (Figure 1D,E). The other biological networks activated were stimulant-dependent. Complete results of the IPA analysis are available in supplementary data (Supplementary Data S1). Interestingly, the biological networks activated in HV were also activated in allo-HSCT recipients, suggesting that both stimulants induced similar canonical pathways in both populations, driven by common upstream regulators, and leading to the activation of similar diseases and biological functions. Taken together, these results suggest that allo-HSCT recipients are able to activate immune responses similarly to HV in response to stimulation, without taking into account activation levels.

Allo-HSCT Patients Harbor Alterations in Inflammation and Regulation Processes

We then evaluated the variation in global gene expression post-stimulation (full gene panel per stimulant). Upon SEB stimulation (Figure 2A), 97/138 (70.3%) and 84/138 (60.9%) genes were differentially expressed compared to the control condition, in HV and allo-HSCT recipients, respectively. After LPS stimulation (Figure 2B), 85/134 (64.9%) and 64/134 (47.8%) genes were differentially expressed in HV and allo-HSCT recipients, respectively. Of note, all genes differentially expressed

Table 1
Characteristics of Allo-HSCT Recipients

	Allo-HSCT recipients (n = 60)
Demographics	
Age (yr), median [IQR]	44.5 [34-60]
Male	34 (57%)
Time from transplantation, months, median [IQR]	6.6 [5.8-8.3]
Hematological and transplant-related characteristics	
Underlying hematological disease*	
Acute myeloid leukemia and related neoplasms	31 (52%)
Myelodysplastic syndromes	8 (13%)
Myeloproliferative neoplasms	1 (2%)
B-lymphoblastic leukemia/lymphoma	11 (18%)
T-lymphoblastic leukemia/lymphoma	2 (3%)
Mature neoplasms: T, NK, or B cells	3 (5%)
Hodgkin lymphoma	1 (2%)
Others	3 (5%)
CR before the engraftment	53 (88%)
Donor type	
Matched related donor	18 (30%)
Matched unrelated donor	23 (38%)
Mismatched unrelated donor	6 (10%)
Haploidentical donor	12 (20%)
Umbilical cord blood	1 (2%)
Stem cell source	
Peripheral blood cells	48 (80%)
Bone marrow	11 (18%)
Conditioning regimen	
MAC	22 (37%)
RIC	38 (63%)
TBI	18 (30%)
Donor and recipient CMV status before transplantation	
D+/R−	9 (15%)
D+/R+	21 (35%)
D−/R−	14 (23%)
D−/R+	16 (27%)
Donor and recipient EBV status before transplantation	
D+/R−	1 (2%)
D+/R+	52 (87%)
D−/R−	2 (3%)
D−/R+	5 (8%)
GvHD	
GvHD prophylaxis	
ATG	34 (57%)
Calcineurin inhibitors	59 (98%)
Mycophenolate mofetil	33 (55%)
Corticosteroids	0 (0%)
Methotrexate	14 (23%)
Post-transplantation cyclophosphamide	23 (38%)
History of GvHD between transplantation and inclusion, n (%)	
Acute GvHD	42 (70%)
Grade I	28
Grade II	12
Grade III	2
Chronic GvHD	8 (13)
Grade I	3
Grade II	3
Grade III	2
GvHD status at inclusion	
No history of GvHD	16 (27%)
Resolved GvHD	23 (38%)
Active GvHD (acute or chronic)	21 (35%)
Immunophenotyping, mean (range)	
Lymphocytes (NV, 1000-2800/μL)	1601 (410-4910)
CD3$^+$ T-lymphocytes (NV, 521-1772/μL)	887 (145-3406)
CD3$^+$ CD4$^+$ T-lymphocytes (NV, 336-1126/μL)	270 (38-876)
Naïve CD4$^+$ (CD45$^+$CCR7$^+$) (NV, 121-456/μL)	30 (0-390)
Central memory CD4$^+$ (CD45RA$^-$CCR7$^+$) (NV, 92-341/μL)	61 (1-211)
Effector memory CD4$^+$ (CD45RA$^-$CCR7$^-$) (NV, 59-321/μL)	157 (4-704)
Differentiated memory CD4$^+$ (CD45RA$^+$CCR7$^-$) (NV, 11-102/μL)	22 (0-226)
CD3$^+$ CD8$^+$ T-lymphocytes (NV, 125-780/μL)	580 (50-2779)
Naïve CD8$^+$ (CD45$^+$CCR7$^+$) (NV, 86-257μL)	39 (0-241)
Central memory CD8$^+$ (CD45RA$^-$CCR7$^+$) (NV, 19-93/μL)	18 (0-127)
Effector memory CD8$^+$ (CD45RA$^-$CCR7$^-$) (NV, 15-162/μL)	252 (0-1517)
Differentiated memory CD8$^+$ (CD45RA$^+$CCR7$^-$) (NV, 39-212/μL)	276 (0-1500)
CD4$^+$/CD8$^+$ ratio (NV, 0.9-6)	0.97 (0.12- 9.07)
CD20$^+$ B-lymphocytes (NV, 64-593/μL)	282 (14-1439)
Immunoglobulin G titers (NV, 7-16 g/L)	8.6 (2.0-20.3)
Post-transplantation immunomodulatory therapy at inclusion	
IS therapy at inclusion#	19 (32%)
IVIG infusion(s)	41 (68%)
Time since last IVIG infusion (mo), median [IQR]	4 [3-6]
DLI	8 (13%)

* Based on 2016 revisions of the World Health Organization classification of myeloid and lymphoid neoplasms; #Immunosuppressive therapies included ciclosporin (n = 9), tacrolimus (n = 4), corticosteroids (n = 8), and ruxolitinib (n = 3).
ATG indicates antithymocyte globulin; CM, central memory; CR, complete remission; D, donor; DM, differentiated memory; DLI, donor lymphocyte infusion; EM, effector memory; IVIG, intravenous immunoglobulins; MAC, myeloablative conditioning; NK, natural killer; NV, normal values; R, recipient; RIC, reduced-intensity conditioning; TBI, total body irradiation.

after LPS or SEB stimulation in allo-HSCT recipients were also differentially expressed in HV. These results highlight that the number of genes associated with innate or adaptive immune responses that are differentially expressed on stimulation is lower in the allo-HSCT population compared to HV. The complete list of gene expression per stimulant and individual are available in supplementary data (Supplementary Data S2).

Volcano plots were then used to identify the genes for which the expression differed significantly between both populations (FDR corrected P adj $< .05$; 2-FC threshold). Post-SEB stimulation (Figure 2C), 20/138 (14%) genes were significantly and differentially expressed between allo-HSCT recipients and HV; the expression of most of them (n = 18) was lower, and the 10 most impacted genes (squares) were involved in immunoregulatory and inflammatory processes (*CCL20, CCL23, IL1A, IL1B, IL1RN, IL10, IL2, IFNG, SOCS3,* and *SPP1*). On LPS

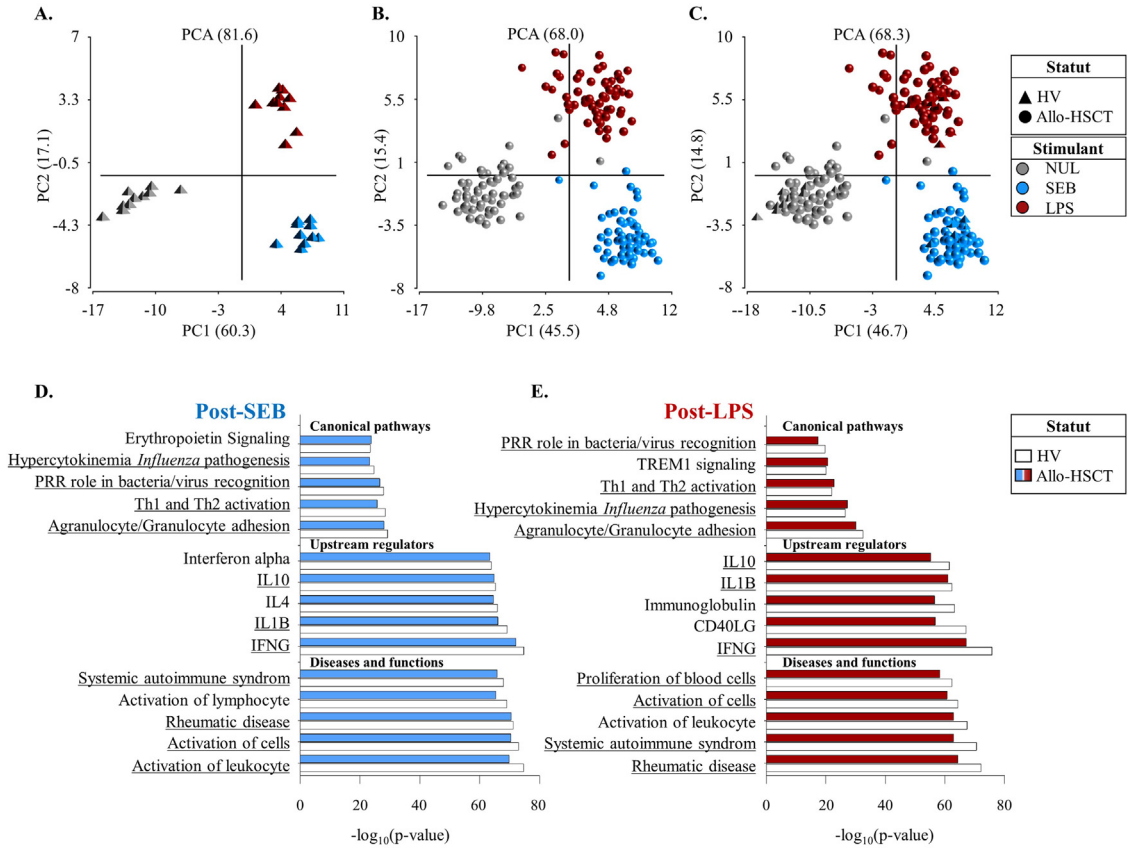

Figure 1. Spatial distribution and biological networks induced by stimulation in healthy volunteers and allo-HSCT recipients. PCA of gene expression data derived from (A) 10 healthy volunteers HV (*triangles*), (B) 60 allo-HSCT patients (*circles*), and (C) both populations. Gene expression data for immune response assessment were obtained post SEB (*blue*) and LPS (*red*) stimulation, as well as within a NUL unstimulated basal condition (*gray*). PCA is projected onto the first 2 principal components and each mark represents an individual transcriptomic profile. Biological networks obtained from IPA for HV (*white bars*) and allo-HSCT recipients (*colored bars*), represented by the top 5 enriched modulated canonical pathways, upstream regulators, and diseases and functions after SEB (D) and LPS (E) stimulation. For canonical pathways and diseases and functions, a −log (*P* value) >2 was set as threshold. For upstream regulators, an overlap *P* value < .05 was set as threshold. Underlined networks correspond to those common between the 2 stimulants.

PC indicates principal component.

stimulation (Figure 2D), 27/135 (20%) genes were significantly and differentially expressed between allo-HSCT and HV; once again, the expression of most of them (n = 25) was lower, and the 10 most impacted genes (squares) were involved in complement cascade and immunoregulatory and inflammatory processes (*C3, CCL19, CCL23, GBP5, IFNG, IP10, MCP1, SERPING1, SPP1,* and *TNFAIP6*). Three genes with a lower expression were common to both SEB and LPS stimulation (*CCL23, IFNG, and SPP1).* This suggests a potential delay in the regulation of immune response and inflammatory processes in the allo-HSCT population at 6 months after transplantation compared to HV. Of note, the 4 genes whose expression was higher in allo-HSCT recipients were only weakly induced after stimulation and thus not biologically relevant. Complete list of differentially expressed gene between HV and allo-HSCT population are available in supplementary data (Supplementary Data S3).

The lower number of DEGs associated with a lower expression level post-stimulation of these DEGs in allo-HSCT recipients led us to compare the enrichment of the biological networks implicated between both populations using an activation score in order to quantitatively evaluate the functional immune response post LPS or SEB challenge. Regardless of the stimulant used and despite the ability of allo-HSCT recipients to activate pathways, upstream regulators, and biological diseases and functions common to HV (Figure 1D,E), the intensity of this activation was significantly lower (*P* adj < .05) in allo-HSCT recipients than in HV for almost all parameters (Figure 2E,F).

Transcriptomic IFA Allows Identification of Immune Functional Alteration Unrevealed by Cellular Counts

Individual immune responses were observed through PCA performed on 3 datasets; the first 2 were obtained after stimulation with either LPS or SEB, respectively, and the last one was obtained by combining the datasets obtained after LPS and SEB stimulation (cumulative condition). Samples projected onto the first 2 PC revealed an overall variability of 39.0%, 40.2%, and 34.2% in the LPS, SEB, and cumulative conditions, respectively. Interestingly, among the 3 datasets we observed a group of allo-HSCT recipients clustered closely to all HV located on the upper right side of PCA, whereas some patients were distant from HV, suggesting distinct transcriptomic profiles (Figure 3A, Figure S1A,B). These observations highlight the heterogeneous nature of the post allo-HSCT immune reconstitution, and suggest that the patients located close to HV have a more advanced functional immune reconstitution than others. To obtain a quantitative characterization of the immune alteration, we calculated, using PCA projection, a Euclidean distance of each allo-HSCT recipient to the centroid of HV population (green square), which serves as a reference

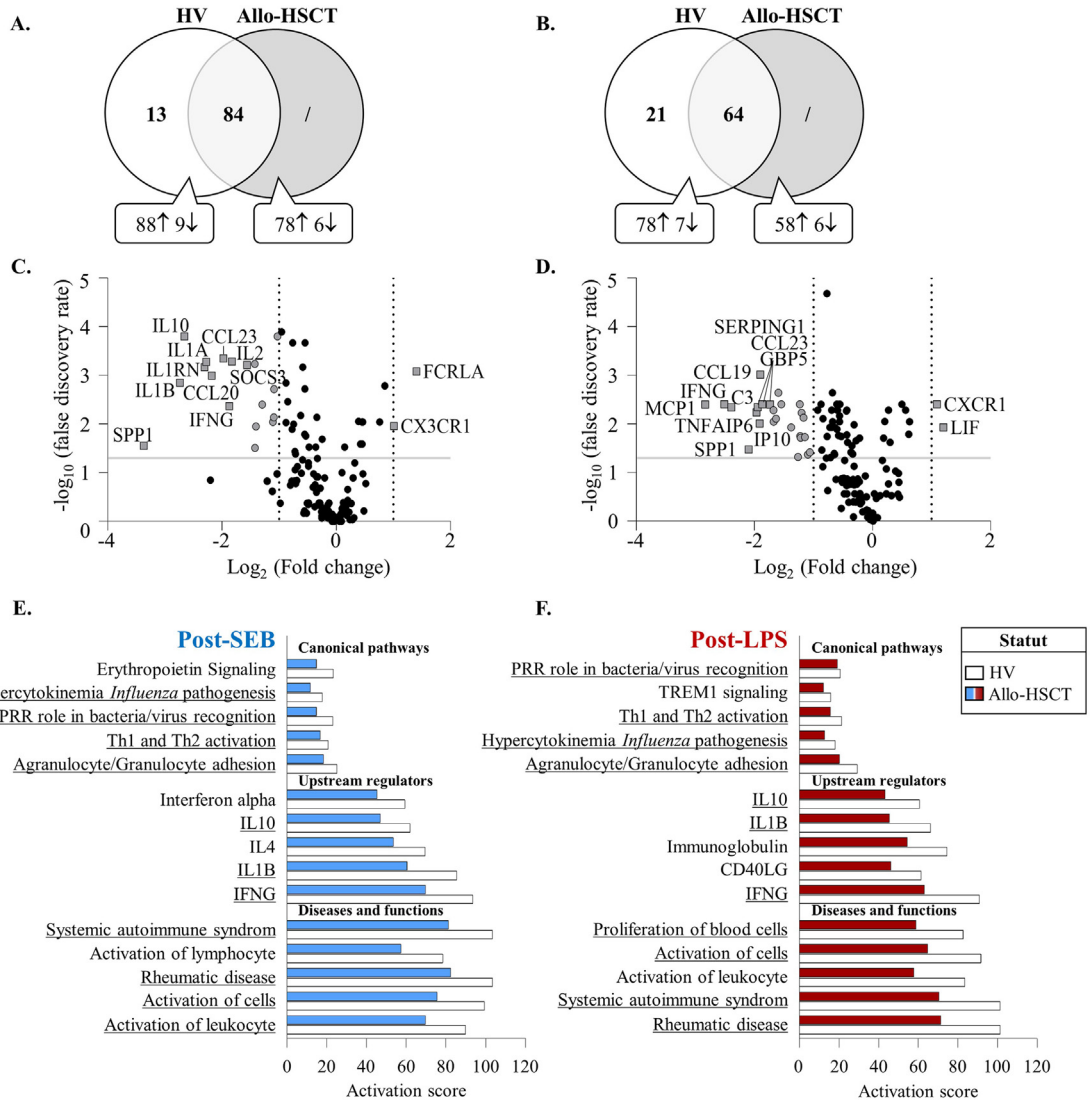

Figure 2. Modulation in the expression of immune response genes post-SEB and post-LPS stimulation in healthy volunteers and allo-HSCT recipients. Venn diagrams of DEG (adjusted $P < .05$ in >75% of tests) between 10 healthy volunteers HV (*white circle*) and 60 allo-HSCT recipients (*gray circle*) after 24 hours of SEB (A) and LPS (B) stimulation. Volcano plots of genes upon SEB (C) and LPS (D) stimulation differing between HV and allo-HSCT population. Fold change (x axis) is plotted against statistical significance (y axis) for each genes. *Black circles* represents genes not found to differ significantly between the HV and allo-HSCT populations. Up- or down-regulated genes with a fold change >2 or <2 and FDR < 0.05 are depicted in gray. The top most impacted genes are detailed and represented as *gray squares*. The biological network activation scores of the top 5 canonical pathways, upstream regulators, and diseases and functions for HV (*white bars*) and allo-HSCT recipients (*colored bars*) on SEB (E) and LPS (F) stimulation. Activation scores for both populations were generated by summing the median expression of component genes for each network. Underlined networks correspond to those common between the two stimulants. PRR indicates pattern recognition receptors; Th, T helper.

value of a functional immune response (Figure 3A, Figure S1A, B). We hypothesized that the greater the distance is, the more allo-HSCT recipients had an altered immune response. We then explored whether 20 of the main biological- or transplant-related factors (age, sex, donor type, stem cell source, underlying disease, GvHD status, etc.) were associated with this Euclidean distance. Interestingly, thresholds classically used to describe an immunosuppression state [50,51] such as a TCD4$^+$ cell count >200 cells/μL or a CD4$^+$/CD8$^+$ ratio >1 did not allow us to identify allo-HSCT recipients with an altered immune response (i.e., with a high Euclidean distance) (Supplementary Table S2). Moreover, among the 20 factors assessed, ongoing immunosuppressive therapy was the only transplantation-related factor statistically associated with an increased Euclidean distance compared to those without, within the cumulative dataset (median [IQR] 15.37 [13.2-20.29] versus 11.34 [5.14-14.39] P adj < .027; Supplementary Table S2). The immunosuppressive drugs used in treated patients (n = 19) were calcineurin inhibitors (cyclosporine [n = 9] and tacrolimus [n= 4]), steroids (n = 8), and ruxolitinib (n = 3).

When comparing patients with ongoing immunosuppressive treatment (n = 19) to those without treatment (n = 41), no significant difference was observed in terms of clinical characteristics. Furthermore, no clinical factor had a significant impact on immunosuppressive therapy use, not even GvHD at inclusion (P adj = .707), because 21% of patients under immunosuppressive treatment did not ever present a GvHD (Supplementary Table S3).

We then assessed whether the immune alteration induced by immunosuppressive treatment could be revealed by immune cell counts, using a large immunophenotyping panel.

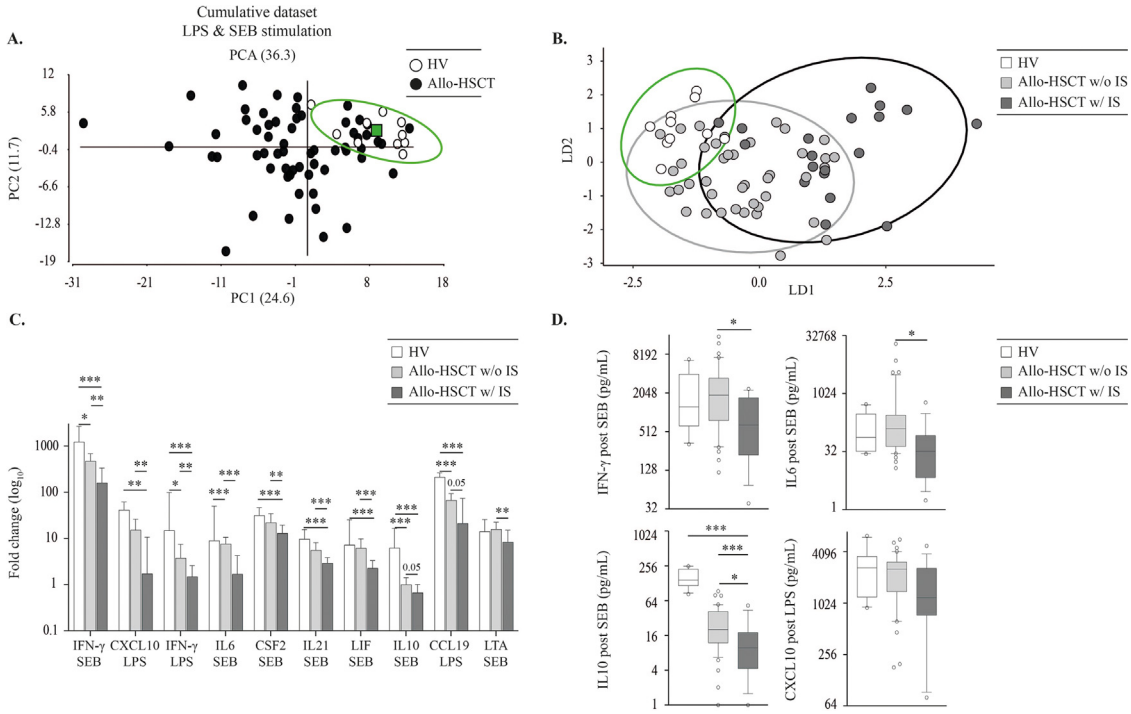

Figure 3. Individual transcriptomic profile of the allo-HSCT population compared to the healthy volunteers population and association with the main disease- and transplant-related factors. (A) PCA of gene expression data derived from 10 healthy volunteers HV (*white circles*) and 60 allo-HSCT patients (*black circles*) on cumulative dataset (gene expression obtained after LPS and after SEB stimulation). Individuals were represented onto the first 2 principal components and each circle represents an individual transcriptomic profile. PCA shows the presence of a specific cluster formed by HV individuals (*green ellipse*), the HV centroid (*green square*) serve as a reference of functional transcriptomic response. (B) LDA representation from the 5 first principal component from (A) (explaining 80% of dataset variability) from 10 HV (*white circles*) and 60 allo-HSCT recipients divided into 2 groups, without (n = 41, *light gray*) or with (n = 19, *dark gray*) ongoing immunosuppressive treatment, the corresponding ellipses are also represented. (C) Expression level of the 10 genes that most contribute to the construction of the first axis of LDA, comparison between HV (*white bars*) and allo-HSCT recipients without (n = 41, *light gray*) or with (n = 19, *dark gray*) immunosuppressive treatment. (D) Comparison of cytokine secretion levels for four genes from LDA analysis (pg/mL) obtained from Truculture supernatants post stimulation and quantified using the ELLA nanofluidic system. *Whisker plots* represent median [Q1-Q3] values. Kruskal-Wallis test with Dunn correction was used for statistical analysis, $P < .05$ is considered significant. IS indicates immunosuppressive.

Table 2
Comparison of Immune Cell Counts of allo-HSCT Recipients According to Immunosuppressive Treatments

Immunophenotyping, (normal value)	No IS treatment (n = 41) Median [IQR]	IS treatment (n = 19) Median [IQR]	*P* Value	*P* Adj
Polynuclear neutrophils (PNN) (NV 2-7.5 × 109/L)	2.8 [2.2-3.8]	4 [3.1-4.4]	.021*	.353
White blood cells (WBC) (NV 4.5-11 × 109/L)	5.4 [4.2-7]	6 [4.8-7.8]	.110	.353
Monocytes (0.2-0.9 × 109/L)	0.5 [0.4-0.7]	0.6 [0.4-0.9]	.187	.390
Absolute lymphocytes (NV, 1-2.8 × 109/L)	1.3 [0.8-2.5]	0.9 [0.7-1.3]	.154	.353
$CD3^+$ T-lymphocytes (NV, 521-1772/μL)	717 [513-1186]	475 [362.5-686.5]	.072	.353
$CD3^+$ $CD4^+$ T-lymphocytes (NV, 336-1126/μL)	287 [151-334]	205 [95-382.5]	.259	.432
Naïve $CD4^+$ ($CD45^+CCR7^+$) (NV, 121-456/μL)	17 [8.5-32]	12 [4-33]	.599	.788
Central memory $CD4^+$ ($CD45RA^-CCR7^+$) (NV, 92-341/μL)	56.5 [22.5-82]	50 [19.5-104]	.795	.864
Effector memory $CD4^+$ ($CD45RA^-CCR7^-$) (NV, 59-321/μL)	143.5 [103.8-208]	98 [64.5-185]	.212	.396
Differentiated memory $CD4^+$ ($CD45RA^+CCR7^-$) (NV, 11-102/μL)	5 [0-29]	3.5 [0.8-20]	.784	.864
$CD3^+$ $CD8^+$ T-lymphocytes (NV, 125-780/μL)	409 [230-790]	250 [141-366.5]	.032*	.353
Naïve $CD8^+$ ($CD45^+CCR7^+$) (NV, 86-257μL)	20.5 [10-54.5]	17.5 [8.2-49]	.749	.864
Central memory $CD8^+$ ($CD45RA^-CCR7^+$) (NV, 19-93/μL)	9.5 [3.2-17]	10 [4-12]	.849	.884
Effector memory $CD8^+$ ($CD45RA^-CCR7^-$) (NV, 15-162/μL)	159 [88-290.8]	107 [62.2-199.8]	.278	.435
Differentiated memory $CD8^+$ ($CD45RA^+CCR7^-$) (NV, 39-212/μL)	223 [88.5-339.5]	72 [22.5-247.5]	.049*	.353
CD4+/CD8+ ratio (NV, 0,9-6)	0.5 [0.4-0.8]	0.8 [0.2-1.3]	.651	.813
$CD2^+$ T-lymphocytes (NV, 800-3000/μL)	785 [614.8-1218.5]	538 [414-813.5]	.090	.353
$CD19^+$ B-lymphocytes (NV, 67-516/μL)	214 [101.2-414.8]	171 [54.5-244.2]	.151	.353
$CD20^+$ B-lymphocytes (NV, 64-593/μL)	213 [98.5-424.5]	168 [54.2-240.8]	.156	.353
$CD21^+$ B-lymphocytes (NV, 67-516/μL)	203 [86.8-390.2]	161.5 [49-230.8]	.139	.353

* Based on 2016 revisions of the World Health Organization classification of myeloid and lymphoid neoplasms.
Immunosuppressive treatments included ciclosporin (n = 9), tacrolimus (n = 4), corticosteroids (n = 8), ruxolitinib (n = 3). Adjusted *P* values were calculated using the Bonferroni correction method and were considered statistically significant if <.05.

In patients with ongoing immunosuppressive treatment compared to those without, no significant difference was observed in terms of immune cell counts (P adj > .53; Table 2). Of note, no significant correlation was observed between Euclidean distance and the lymphocyte subset counts (Spearman P adj > .12). These results suggest an added value of transcriptomic IFA to depict immune reconstitution in addition to the cellular counts routinely used.

Next, to precisely characterize which transcriptomic features allow us to distinguish allo-HSCT recipients with immunosuppressive treatment, without immunosuppressive treatment, and HV samples, we used an LDA approach (Figure 3B). As observed, the 3 groups are distinctly separated along the first axis of the LDA. We then identified the top 10 genes that contribute to the construction of this axis: *CCL19, CSF2, CXCL10, IFNG, IL10, IL21, IL6, LIF,* and *LTA*. These genes were mainly obtained after SEB (7/10) rather than LPS (3/10) stimulation and had a significantly lower expression (P adj < .05) in allo-HSCT recipients with an ongoing immunosuppressive treatment when compared to those without treatment or to the HV population (Figure 3C). Of note, similar results were also observed for the proteins encoded by 4 of these genes, with an at least 2-fold lower secretion in patients with immunosuppressive treatments compared to those without, for IFN-γ, IL6, IL10 after SEB, and CXCL10 after LPS stimulation (Figure 3D). Overall, these results highlight the potential of transcriptomic IFA for the individual assessment of immune function and to reveal specific immune alterations.

Reactivation of Herpesviridae *Was Associated With a Lower Expression of* CCL4 *and* CCL3 *Genes*

Finally, because immune function is closely related to infectious complications, we next assessed the immune transcriptomic profile of allo-HSCT recipients according to ongoing infections.

During the first 6 months after transplantation, 56/60 (93.3%) patients had at least 1 notable infectious episode. A total of 188 infectious episodes were recorded, 57 of which required a specific treatment. Viral infections were the most prominent (51%), especially *Herpesviridae* reactivations with EBV (36%), CMV (19%), or HHV-6 (11%). This observation led us to assess a possible association between immune function and viral reactivation.

Within the 14 days before or after inclusion, 19 (32%) allo-HSCT recipients experienced at least 1 infectious episode. Infectious episodes were exclusively related to *Herpesviridae* reactivation with a large prevalence of asymptomatic EBV reactivation (17/19, 89%), which did not require any specific treatment. Of note, almost all infectious episodes occurred within the 14 days before whole-blood sampling (1/19 at day 5 and 18/19 with an ongoing chronic lasting EBV or HHV-6 reactivation). No significant difference (P adj > .99) was found between recipients with (n = 19) or without (n = 41) infectious episodes, in terms of demographic and transplant-related-characteristics (Table 3). In terms of quantitative cell count measurements, the comparison between patients with and without ongoing *Herpesviridae* reactivation revealed also no significant differences (P adj >.99). Strikingly, classical thresholds used in clinical routine were not useful to discriminate patients with or without infectious episodes because 12/19 (63%) and 25/41 (61%) had a TCD4+ count >200 cells/μL (P > .99), and 3/19 (16%) and 12/41 (29%) had a $CD4^+/CD8^+$ ratio >1 (P adj = .35), respectively.

After LPS or SEB stimulation, 17 genes were found to be differentially expressed (FDR Benjamini-Hochberg corrected P adj < .05; 2-FC threshold) between patients with and without *Herpesviridae* reactivation. A supervised analysis revealed a lower expression of these 17 genes after stimulation in allo-HSCT recipients with *Herpesviridae* reactivation compared to those without (Figure 4A). The 4 genes whose expression were the most significantly lower (P adj < .01) in recipients with *Herpesviridae* reactivation compared to those without were *CCL4* (post-LPS, FC 6.9 versus 23.3, post-SEB, FC 12.6 versus 30.2), *CCL3* (post-LPS, FC 23.2 versus 53.7), *SLAMF7* (post-LPS, FC 8.8 versus 19.4), and *CD274* (post-LPS, FC 10.4 versus 30.4; Figure 4B). Finally, ROC curves representation and calculation of respective AUC were performed to evaluate the discriminating power of post-stimulation genes expression compared to classical quantitative cell counts among infected and uninfected allo-HSCT recipients. AUC obtained with genes expression after stimulation was at least >0.79 whereas AUC obtained through cell counts was significantly lower, with a maximum of 0.69 [0.54-0.84] for CD4+/CD8+ ratio (Figure 4C).

DISCUSSION

The present analysis based on a whole-blood IFA, provides a description of the immune functional state of a cohort of allo-HSCT recipients, at 6 months after transplantation. This late post-transplantation timepoint is a pivotal period for allo-HSCT recipients, as immunosuppressive treatment is weaned, prophylactic therapies are adapted, and the revaccination schedule is initiated [13]. Furthermore, although innate immunity is quantitatively normal and lymphocyte counts representing adaptive immunity are only mildly or moderately abnormal, their functionality remains to be characterized.

The use of whole-blood IFA enabled to demonstrate the ability of allo-HSCT recipients to activate the same immune networks than HV in response to immune challenges. Nevertheless, allo-HSCT recipients had a fewer number of DEG than HV, leading to an immune response of weaker intensity on both SEB and LPS stimulation. Genes with a lower expression were mainly involved in immunoregulatory and inflammatory processes. Indeed, post-SEB stimulation, the genes with the most significant lower expression were *IL2*, a marker of T-cell activation [52], *IL1*-related genes, and *IL10*, both regulating inflammatory and immune responses [40,53]. After LPS stimulation, an altered expression of *C3* was observed, a gene related to the activation of the complement system acting as a functional bridge between innate and adaptive immunity that leads to the production of proinflammatory molecules [54,55]. A reduced expression of *MCP1* (also known as *CCL2*) was highlighted. This gene encodes for a chemoattractant of myeloid and lymphoid cells during the inflammatory process and acts as an effector of T-cell differentiation [56], previously reported to be activated by inflammatory stimuli such as LPS [57]. Furthermore, the observed lower expression of *IFNG* with both stimulants potentially reflects a slower functional reconstitution of natural killer or T-cells, the main IFN-γ producing cells [58]. The lower expression of genes identified through volcano plotting explained the weaker biological networks' intensity in allo-HSCT recipients compared to HV. The canonical pathways altered in allo-HSCT recipients were mainly linked to the recognition of infectious agents and the induction of inflammatory reaction or adaptive response. Altogether, the genes with an altered expression were associated with defects in key biological functions, not necessarily specific of a cellular component or system, but involved in many immune response processes. Except for donor lymphocyte infusions, no immune-boosting strategy after allo-HSCT is routinely performed. However, as recently described [59,60], immune-

Table 3
Characteristics of Allo-HSCT Recipients According to Herpersviridae Infection Status

Herpesviridae infection	Presence (n = 19)	Absence (n = 41)	*P* Value	*P* adj
Etiology		NA	NA	NA
EBV	17			
CMV (including one combined with EBV)	2			
HHV6	1			
Demographics				
Age (yr), median [IQR]	41 [28-57]	45 [35-63]	.164	1.000
Male	11 (58%)	23 (56%)	.881	1.000
Time from transplantation, months, median [IQR]	6.4 [5.8-7.6]	7.4 [5.8-8.6]	.353	1.000
Hematological and transplant-related characteristics				
Underlying hematological disease*			.859	1.000
Acute myeloid leukemia and related neoplasms	9 (47%)	22 (54%)		
Myelodysplastic syndromes	3 (16%)	5 (12%)		
Myeloproliferative neoplasms	0 (0%)	1 (2%)		
B-lymphoblastic leukemia/lymphoma	5 (26%)	6 (15%)		
T-lymphoblastic leukemia/lymphoma	0 (0%)	2 (5%)		
Mature neoplasms: T, NK, or B cells	1 (5%)	2 (5%)		
Hodgkin lymphoma	1 (5%)	0 (0%)		
Others	0 (0%)	3 (7%)		
CR before the engraftment	16 (84%)	37 (90%)	.323	1.000
Donor type			.810	1.000
Matched related donor (MRD)	4 (21)	14 (34)		
Matched unrelated donor (MUD)	9 (90)	14 (74)		
Mismatched unrelated donor (MMUD)	1 (10)	5 (26)		
Haploidentical donor	5 (26)	7 (17)		
Umbilical cord blood (UCB)	0 (0)	1 (2)		
Stem cell source	—	—	1.000	1.000
Peripheral blood cells	15 (79)	33 (81)		
Bone marrow	4 (21)	7 (17)		
Conditioning regimen	—	—		
MAC	11 (58)	27 (66)	1.000	1.000
RIC	8 (42)	14 (34)		
TBI	7 (37)	11 (27)		
GvHD				
GvHD prophylaxis				
ATG	14 (74%)	20 (49%)	.095	1.000
Calcineurin inhibitors	19 (100%)	40 (98%)	1.000	1.000
Mycophenolate mofetil	12 (63%)	21 (51%)	.558	1.000
Corticosteroids	0 (0%)	0 (0%)	NA	NA
Methotrexate	5 (26%)	9 (22%)	.750	1.000
Cyclophosphamide	7 (37%)	16 (39%)	1.000	1.000
History of GvHD between transplantation and inclusion				
Acute GvHD	15 (79%)	27 (66%)	.375	1.000
Chronic GvHD	3 (16%)	5 (12%)	.699	1.000
GvHD status at inclusion				
No history of GvHD	4 (21%)	12 (29%)	.503	1.000
Resolved GvHD	8 (42%)	15 (37%)	.683	1.000
Active GvHD (acute or chronic)	7 (37%)	14 (34%)	.839	1.000
Immunophenotyping, mean (range)				
Lymphocytes (NV, 1000-2800/μL)	1869 (490-4910)	1473 (410-4650)	.377	1.000
$CD3^+$ T-lymphocytes (NV, 521-1772/μL)	1081 (188-3406)	797 (145-2910)	.539	1.000
$CD3^+$ $CD4^+$ T-lymphocytes (NV, 336-1126/μL)	273 (38-785)	269 (60-876)	.697	1.000
Naïve $CD4^+$ ($CD45^+CCR7^+$) (NV, 121-456/μL)	20.5 (0-121)	34.3 (1-390)	.165	1.000
Central memory $CD4^+$ ($CD45RA^-CCR7^+$) (NV, 92-341/μL)	49.7 (1-140)	65.4 (1-211)	.266	1.000
Effector memory $CD4^+$ ($CD45RA^-CCR7^-$) (NV, 59-321/μL)	179.5 (13-704)	147.8 (4-368)	.934	1.000
Differentiated memory $CD4^+$ ($CD45RA^+CCR7^-$) (NV, 11-102/μL)	15.0 (0-95)	25.3 (0-226)	.187	1.000
$CD3^+$ $CD8^+$ T-lymphocytes (NV, 125-780/μL)	776 (60-2779)	489 (50-2422)	.139	1.000
Naïve $CD8^+$ ($CD45^+CCR7^+$) (NV, 86-257μL)	28.8 (0-156)	44.3 (2-241)	.083	1.000

(*continued*)

Table 3 (*Continued*)

Herpesviridae infection	Presence (n = 19)	Absence (n = 41)	*P* Value	*P* adj
Central memory CD8$^+$ (CD45RA$^-$CCR7$^+$) (NV, 19-93/μL)	19.8 (0-97)	17.7 (0-127)	.741	1.000
Effector memory CD8$^+$ (CD45RA$^-$CCR7$^-$) (NV, 15-162/μL)	418 (0-1517)	177 (1-843)	.100	1.000
Differentiated memory CD8$^+$ (CD45RA$^+$CCR7$^-$) (NV, 39-212/μL)	317 (0-1102)	258 (0-1500)	.315	1.000
CD4$^+$/CD8$^+$ ratio (NV, 0.9-6)	0.55 (0.17-2.33)	1.17 (0.12-9.07)	.019*	1.000
CD19$^+$ B-lymphocytes (NV, 64-593/μL)	274 (14-1435)	289 (15-1299)	.540	1.000
Post-transplantation immunomodulatory therapy at inclusion				
IS therapy at inclusion	8 (42%)	11 (27%)	.376	1.000
IVIG infusion(s)	17 (89%)	24 (59%)	.003*	1.000
DLI	3 (16%)	5 (12%)	.703	1.000

HHV6 indicates human herpesvirus 6.
Immunosuppressive therapies included ciclosporin (n = 9), tacrolimus (n = 4), corticosteroids (n = 8), and ruxolitinib (n = 3).
* Based on 2016 revisions of the World Health Organization classification of myeloid and lymphoid neoplasms.

based approaches, such as cellular therapies and soluble factors, are currently under study.

The assessment of individual post-stimulation transcriptomic profiles revealed that immune reconstitution in allo-HSCT recipients is highly heterogeneous. Some allo-HSCT recipients displayed a transcriptomic profile similar to that observed in HV, suggesting a more advanced process of immune reconstitution. Interestingly, the patients with the most distinct transcriptomic responses compared to HV were mainly allo-HSCT recipients with an ongoing immunosuppressive treatment, independently of any confounding clinical factor. These patients were characterized by a lower expression of key genes of the immune response such as *CSF2, IFNG, IL10, IL21* or *IL6* resulting for some of them in a lower secretion of related encoded proteins. This is in line with previous data reporting the effect of immunosuppressive treatments, such as calcineurin inhibitors, the most used class of immunosuppressive drugs in the present study, which affect NFAT pathway-related gene expression and protein secretion [61–65]. In addition, no association between a specific

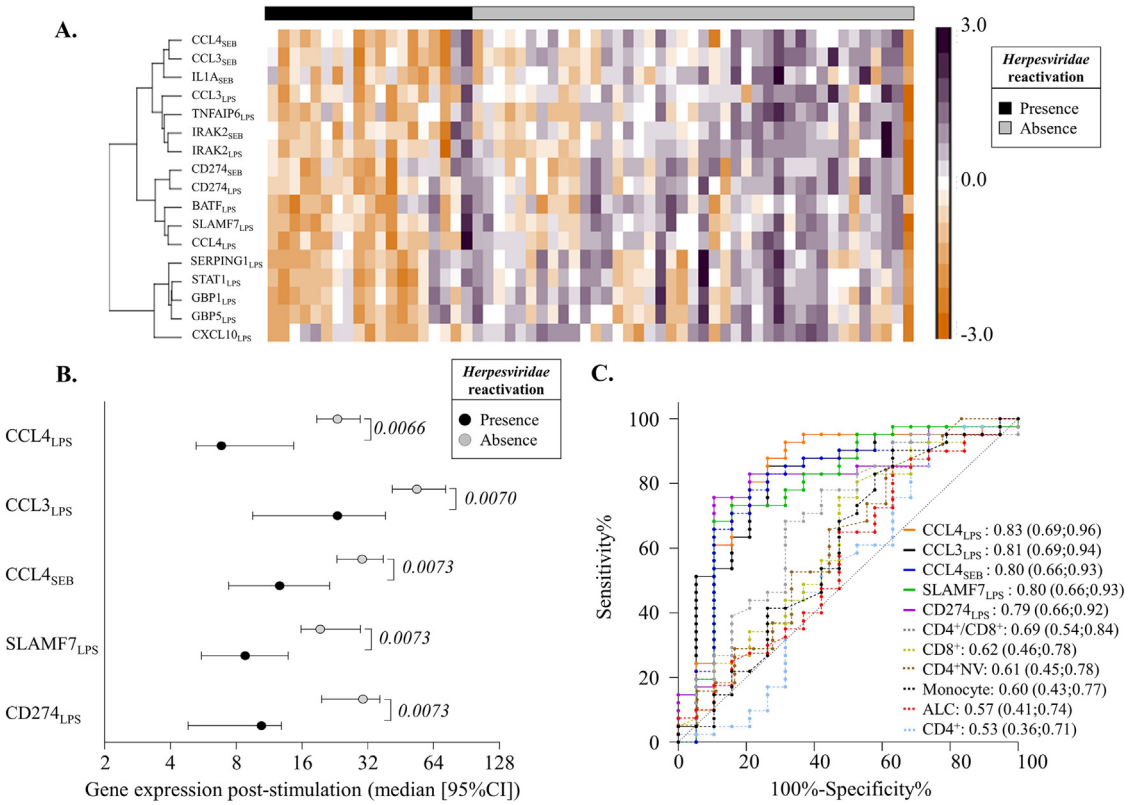

Figure 4. Transcriptomic immune profile according to the presence or absence of recent viral infectious episodes and main genes impacted. Heatmap of gene expression profiles (A) from supervised analysis (Euclidean distances matrix with Ward's methods) generated by scaling and centering log10-transformed gene expression FC and based on the 17 genes with the highest significant ($P < .05$) differences in expression between recipients with (n = 19) and without infectious episodes (n = 41). Genes clustering is indicated by a dendogram tree for selected genes (*left*). The colored bars at the top of the heatmap represent the membership of recipients in groups with (*black*) or without (*gray*) infectious episodes. (B) Graphical plot representing the expression of the top 5 most DEG (FC > 2 and $P < .01$) within allo-HSCT recipients with (n = 19) or without infectious episodes (n = 41), median and [95% CI] values are represented by *dots* and *lines*, respectively. (C) ROC curves obtained from the comparison between allo-HSCT recipients with (n = 19) and without infectious episodes (n = 41) regarding the 5 most DEG and quantitative cell counts from the large immunophenotyping panel. AUC [95%CI] is indicated for each parameter. CI indicates confidence interval.

transcriptomic profile and other major clinical characteristics, such as GvHD status at inclusion, was found. Regarding immune cell counts, those classically quantified to assess post-transplantation immune reconstitution, such as $TCD4^+$ cell count and $CD4^+$ /$CD8^+$ ratio, were not able to reveal these alterations [50,51].

Several studies have shown the interest of evaluating the immune response using a post-stimulation approach with TruCulture tubes in healthy populations [26,39,66], in an infectious context [27,67], and in the context of solid organ transplantation [68]. In the allo-HSCT setting, a recent study revealed the magnitude and the heterogeneity of functional immune responses reflected by the variation in cytokine responses before and early after transplantation [28], a second one also used functional analysis to describe immune reconstitution [69]. Although previous studies have described the heterogeneity of allo-HSCT recipients regarding quantitative parameters of immune reconstitution [70], this is the first, to the best of our knowledge, to report post-stimulation transcriptional immunoprofiling in the late post-transplant period in allo-HSCT recipients. The results herein highlight that the information provided by immune function assessment is different and complementary to that captured by the quantitative measurement of circulating immune cells.

Finally, we were able to identify a set of genes associated with ongoing infectious episodes, only related in this study to *Herpesviridae* reactivation, which are frequent events in immunocompromised populations [71]. A recent study described an altered immune response against *Herpesviridae* in older people [72]. Interestingly, the state of immunosenescence occurring in older people could be in some way compared to what is observed in allo-HSCT recipients, notably regarding phenotypes of immune cells which are mainly made up of memory phenotypes and highly restricted to naive phenotypes or effector cells. In the present study, allo-HSCT recipients with *Herpesviridae* reactivation presented a significantly lower expression of *CCL3* and *CCL4* genes post-stimulation. These chemokines are potent chemoattractants of innate and adaptive immune cells during inflammatory processes, and their dysregulation has been linked to an increased susceptibility to infection [73,74], or associated to the presence of ongoing viral reactivation [75]. Interestingly, allo-HSCT recipients with *Herpesviridae* reactivation had again no specific clinical features. Quantitative biomarkers used in routine practice failed to discriminate patients with or without infections, notably T-cell counts (total or naïve), which are described as key controllers of infections after HSCT [76–78]. Altogether, the present results confirm the potential added-value of IFA in providing additional information on immunocompetence in the allo-HSCT setting, as previously suggested [6,28,79]. In the current state, this IFA transcriptomic tool is not yet suitable for application in the clinical setting, mainly due to the complexity and time required for interpreting the results. Nevertheless, it paves the way to a new approach regarding the assessment of individual immune capacities. Indeed, deciphering immune signatures through transcriptomic analysis might help develop personalized precision medicine. In the context of allo-HSCT, such tests, reflecting the functional immune status, could allow us to better characterize immune reconstitution to optimize prophylactic strategies.

There are some limitations to this study. In this pilot study, performed at a single institution, the number of patients included was limited, and the results need to be confirmed. Immune function assessment herein is only representative of the selected stimuli (LPS and SEB). Functional immune reconstitution was studied at a single timepoint, but the ongoing follow-up of the cohort should enable to provide dynamic data regarding the kinetics of immune reconstitution overtime. The biological network assessment might be biased by the custom gene-panel. We have also chosen to use a standardized whole blood IFA to limit the technical variability and to increase applicability in the clinical setting. This choice, however, did not allow us to associate the biological network alterations observed with a specific immune cell type. To do so, it would be necessary to perform stimulation assays on isolated sorted cells. Finally, it cannot be excluded that the important inter-individual variability observed, with no evident link to clinical characteristics, is due to the heterogeneity of allo-HSCT recipients included in the study. Indeed, no specific selection was applied in terms of participants who were representative of the HSCT patient population at our institution, but this might lead to a lack of power.

In conclusion, this first descriptive analysis of the transcriptomic profile of allo-HSCT recipients demonstrates the added value of IFA for deciphering different immune profile signatures that could not be captured by quantification of immune cell counts, currently used in the clinical setting. Besides the interest in assessing individual immune function profiles, the present results pave the way to longitudinal studies, which could assess the predictive value of this tool in terms of relevant clinical post-transplantation outcomes, especially infectious episodes and GvHD, and could ultimately contribute to personalized precision medicine.

Conflict of interest statement: K.B.P., G.O., and M.Bod are employees of bioMérieux SA.

SUPPLEMENTARY MATERIALS

Supplementary material associated with this article can be found in the online version at doi:10.1016/j.jtct.2022.10.025.

REFERENCES

1. Ljungman P, Bregni M, Brune M, et al. Allogeneic and autologous transplantation for haematological diseases, solid tumours and immune disorders: current practice in Europe 2009. *Bone Marrow Transplant*. 2010;45:219–234.
2. Copelan EA. Hematopoietic stem-cell transplantation. *N Engl J Med*. 2006;354:1813–1826.
3. Bosch M, Khan FM, Storek J. Immune reconstitution after hematopoietic cell transplantation. *Curr Opin Hematol*. 2012;19:324–335.
4. Ogonek J, Kralj Juric M, Ghimire S, et al. Immune reconstitution after allogeneic hematopoietic stem cell transplantation. *Front Immunol*. 2016;7:507.
5. Carson K, Mehta J, Singhal S. Reimmunization after stem cell transplantation. In: Treleaven J, Barrett AJ, eds. *Hematopoietic Stem Cell Transplantation in Clinical Practice*. 2009;363-368.
6. de Silva HD, Ffrench RA, Korem M, et al. Contemporary analysis of functional immune recovery to opportunistic and vaccine-preventable infections after allogeneic haemopoietic stem cell transplantation. *Clin Transl Immunol*. 2018;7(10):e1040.
7. Storek J. Immunological reconstitution after hematopoietic cell transplantation – its relation to the contents of the graft. *Expert Opin Biol Ther*. 2008;8:583–597.
8. Bejanyan N, Brunstein CG, Cao Q, et al. Delayed immune reconstitution after allogeneic transplantation increases the risks of mortality and chronic GVHD. *Blood Adv*. 2018;2:909–922.
9. Gratwohl A. Hematopoietic stem cell transplantation: a global perspective. *JAMA*. 2010;303:1617.
10. Pidala J. Graft-vs-host disease following allogeneic hematopoietic cell transplantation. *Cancer Control*. 2011;18:268–276.
11. Giaccone L, Felicetti F, Butera S, et al. Optimal delivery of follow-up care after allogeneic hematopoietic stem-cell transplant: improving patient outcomes with a multidisciplinary approach. *J Blood Med*. 2020;11:141–162.
12. Sahin U, Toprak SK, Atilla PA, Atilla E, Demirer T. An overview of infectious complications after allogeneic hematopoietic stem cell transplantation. *J Infect Chemother*. 2016;22:505–514.
13. Tomblyn M, Chiller T, Einsele H, et al. Guidelines for preventing infectious complications among hematopoietic cell transplantation recipients: a global perspective. *Biol Blood Marrow Transplant*. 2009;15:1143–1238.

14. Gratwohl A, Brand R, Frassoni F, et al. Cause of death after allogeneic haematopoietic stem cell transplantation (HSCT) in early leukaemias: an EBMT analysis of lethal infectious complications and changes over calendar time. *Bone Marrow Transplant*. 2005;36:757–769.
15. Styczyński J, Tridello G, Koster L, et al. Death after hematopoietic stem cell transplantation: changes over calendar year time, infections and associated factors. *Bone Marrow Transplant*. 2020;55:126–136.
16. Lin R, Liu Q. Diagnosis and treatment of viral diseases in recipients of allogeneic hematopoietic stem cell transplantation. *J Hematol Oncol*. 2013;6:94.
17. Ljungman P, de la Camara R, Cordonnier C, et al. Management of CMV, HHV-6, HHV-7 and Kaposi-sarcoma herpesvirus (HHV-8) infections in patients with hematological malignancies and after SCT. *Bone Marrow Transplant*. 2008;42:227–240.
18. Styczynski J, Reusser P, Einsele H, et al. Management of HSV, VZV and EBV infections in patients with hematological malignancies and after SCT: guidelines from the Second European Conference on Infections in Leukemia. *Bone Marrow Transplant*. 2009;43:757–770.
19. Kowalski RJ, Zeevi A, Mannon RB, Britz JA, Carruth LM. Immunodiagnostics: evaluation of functional T-cell immunocompetence in whole blood independent of circulating cell numbers. *J Immunotoxicol*. 2007;4:225–232.
20. Luo Y, Xie Y, Zhang W, et al. Combination of lymphocyte number and function in evaluating host immunity. *Aging*. 2019;11:12685–12707.
21. Janetzki S, Schaed S, Blachere NEB, et al. Evaluation of Elispot assays: influence of method and operator on variability of results. *J Immunol Methods*. 2004;291(1–2):175–183.
22. Smith SG, Joosten SA, Verscheure V, et al. Identification of major factors influencing ELISpot-based monitoring of cellular responses to antigens from Mycobacterium tuberculosis. *PLoS ONE*. 2009;4(11):e7972.
23. Smith JG, Liu X, Kaufhold RM, Clair J, Caulfield MJ. Development and validation of a gamma interferon ELISPOT assay for quantitation of cellular immune responses to varicella-zoster virus. *Clin Diagn Lab Immunol*. 2001;8:871.
24. Vogt R, Schulte PA. Evaluation of immune responses. *IARC Sci Publ*. 2011:(163):215–239.
25. Albert-Vega C, Tawfik DM, Trouillet-Assant S, et al. Immune functional assays, from custom to standardized tests for precision medicine. *Front Immunol*. 2018;9:2367.
26. Duffy D, Rouilly V, Libri V, et al. Functional analysis via standardized whole-blood stimulation systems defines the boundaries of a healthy immune response to complex stimuli. *Immunity*. 2014;40:436–450.
27. Albert Vega C, Oriol G, Bartolo F, et al. Deciphering heterogeneity of septic shock patients using immune functional assays: a proof of concept study. *Sci Rep*. 2020;10:16136.
28. Gjærde LK, Brooks PT, Andersen NS, et al. Functional immune reconstitution early after allogeneic haematopoietic cell transplantation: a comparison of pre- and post-transplantation cytokine responses in stimulated whole blood. *Scand J Immunol*. 2021;94(1):e13042.
29. Bohannon JK, Hernandez A, Enkhbaatar P, Adams WL, Sherwood ER. The immunobiology of toll-like receptor 4 agonists: from endotoxin tolerance to immunoadjuvants. *Shock*. 2013;40:451–462.
30. Raetz CRH, Whitfield C. Lipopolysaccharide endotoxins. *Annu Rev Biochem*. 2002;71:635–700.
31. Fries BC, Varshney AK. Bacterial toxins—staphylococcal enterotoxin B. *Microbiol Spectr*. 2013;1(2). https://doi.org/10.1128/microbiolspec.AID-0002-2012.
32. Pinchuk IV, Beswick EJ, Reyes VE. Staphylococcal enterotoxins. *Toxins*. 2010;2:2177–2197.
33. Conrad A, Boccard M, Valour F, et al. VaccHemInf project: protocol for a prospective cohort study of efficacy, safety and characterisation of immune functional response to vaccinations in haematopoietic stem cell transplant recipients. *BMJ Open*. 2019;9(2): e026093.
34. Cordonnier C, Einarsdottir S, Cesaro S, et al. Vaccination of haemopoietic stem cell transplant recipients: guidelines of the 2017 European Conference on Infections in Leukaemia (ECIL 7). *Lancet Infect. Dis*. 2019;19(6): e200–e212.
35. Ljungman P, de la Camara R, Robin C, et al. Guidelines for the management of cytomegalovirus infection in patients with haematological malignancies and after stem cell transplantation from the 2017 European Conference on Infections in Leukaemia (ECIL 7). *Lancet Infect.Dis*. 2019;19(8):e260–e272.
36. Styczynski J, van der Velden W, Fox CP, et al. Management of Epstein-Barr virus infections and post-transplant lymphoproliferative disorders in patients after allogeneic hematopoietic stem cell transplantation: Sixth European Conference on Infections in Leukemia (ECIL-6) guidelines. *Haematologica*. 2016;101:803–811.
37. Ogata M, Satou T, Kadota J, et al. Human herpesvirus 6 (HHV-6) reactivation and HHV-6 encephalitis after allogeneic hematopoietic cell transplantation: a multicenter, prospective study. *Clin Infect Dis*. 2013;57:671–681.
38. Ward KN, Hill JA, Hubacek P, et al. Guidelines from the 2017 European Conference on Infections in Leukaemia for management of HHV-6 infection in patients with hematologic malignancies and after hematopoietic stem cell transplantation. *Haematologica*. 2019;104:2155–2163.
39. Urrutia A, Duffy D, Rouilly V, et al. Standardized whole-blood transcriptional profiling enables the deconvolution of complex induced immune responses. *Cell Rep*. 2016;16:2777–2791.
40. Goytain A, Ng T. NanoString nCounter technology: high-throughput RNA validation. *Methods Mol Biol*. 2020;2079:125–139.
41. Ovesná J, Kučera L, Vaculová K, et al. Validation of the β-amy1 transcription profiling assay and selection of reference genes suited for a RT-qPCR assay in developing Barley caryopsis. *PLoS ONE*. 2012;7(7):e41886.
42. Zhang J, Xie W, Yu X, et al. Selection of suitable reference genes for RT-qPCR gene expression analysis in Siberian wild rye (Elymus sibiricus) under different experimental conditions. *Genes*. 2019;10:451.
43. Nagy NA, Németh Z, Juhász E, et al. Evaluation of potential reference genes for real-time qPCR analysis in a biparental beetle, *Lethrus apterus* (Coleoptera: Geotrupidae). *PeerJ*. 2017;5:e4047.
44. Sarker N, Fabijan J, Emes RD, et al. Identification of stable reference genes for quantitative PCR in koalas. *Sci Rep*. 2018;8:3364.
45. Krämer A, Green J, Pollard J, Tugendreich S. Causal analysis approaches in Ingenuity Pathway Analysis. *Bioinform*. 2014;30:523–530.
46. Meng T, Chen H, Sun M, et al. Identification of differential gene expression profiles in placentas from preeclamptic pregnancies versus normal pregnancies by DNA microarrays. *OMICS*. 2012;16:301–311.
47. Lopez J, Mommert M, Mouton W, et al. Early nasal type I IFN immunity against SARS-CoV-2 is compromised in patients with autoantibodies against type I IFNs. *J Exp Med*. 2021;218(10): e20211211.
48. Jombart T, Ahmed I. adegenet 1.3-1: new tools for the analysis of genome-wide SNP data. *Bioinformatics*. 2011;27:3070–3071.
49. Dekker L, de Koning C, Lindemans C, Nierkens S. Reconstitution of T cell subsets following allogeneic hematopoietic cell transplantation. *Cancers*. 2020;12:1974.
50. Stein DS, Korvick JA, Vermund SH. CD4+ lymphocyte cell enumeration for prediction of clinical course of human immunodeficiency virus disease: a review. *J Infect Dis*. 1992;165:352–363.
51. Margolick JB, Gange SJ, Detels R, et al. Impact of inversion of the CD4/CD8 ratio on the natural history of HIV-1 infection. *J Acquir Immune Defic Syndr*. 2006;42:620–626.
52. Boyman O, Sprent J. The role of interleukin-2 during homeostasis and activation of the immune system. *Nat Rev Immunol*. 2012;12:180–190.
53. Dinarello CA. Overview of the IL-1 family in innate inflammation and acquired immunity. *Immunol Rev*. 2018;281:8–27.
54. Dunkelberger JR, Song W-C. Complement and its role in innate and adaptive immune responses. *Cell Res*. 2010;20:34–50.
55. Carroll MC. The complement system in regulation of adaptive immunity. *Nat Immunol*. 2004;5:981–986.
56. Luther SA, Cyster JG. Chemokines as regulators of T cell differentiation. *Nat Immunol*. 2001;2:102–107.
57. Gschwandtner M, Derler R, Midwood KS. More than just attractive: how CCL2 influences myeloid cell behavior beyond chemotaxis. *Front Immunol*. 2019;10:2759.
58. Castro F, Cardoso AP, Gonçalves RM, Serre K, Oliveira MJ. Interferon-gamma at the crossroads of tumor immune surveillance or evasion. *Front Immunol*. 2018;9:847.
59. Yanir A, Schulz A, Lawitschka A, Nierkens S, Eyrich M. Immune reconstitution after allogeneic haematopoietic cell transplantation: from observational studies to targeted interventions. *Front Pediatr*. 2022;9: 786017.
60. de Koning C, Plantinga M, Besseling P, Boelens JJ, Nierkens S. Immune reconstitution after allogeneic hematopoietic cell transplantation in children. *Biol Blood Marrow Transplant*. 2016;22:195–206.
61. Sommerer C, Meuer S, Zeier M, Giese T. Calcineurin inhibitors and NFAT-regulated gene expression. *Clin Chim Acta*. 2012;413(17–18):1379–1386.
62. Tsuda K, Yamanaka K, Kitagawa H, et al. Calcineurin Inhibitors Suppress Cytokine Production from Memory T Cells and Differentiation of Naïve T Cells into Cytokine-Producing Mature T Cells. *PLoS ONE*. 2012;7(2): e31465.
63. Pacocha SE, Oriente A, Huang S-K, Essayan DM. Regulation of antigen-induced human T-lymphocyte responses by calcineurin antagonists. *J. Allergy Clin. Immunol*. 1999;104(4):828–835.
64. Kim H-P, Korn LL, Gamero AM, Leonard WJ. Calcium-dependent activation of interleukin-21 gene expression in T cells. *J Biol Chem*. 2005;280:25291–25297.
65. Bremer S, Vethe NT, Skauby M, et al. NFAT-regulated cytokine gene expression during tacrolimus therapy early after renal transplantation: NFAT-regulated cytokine gene expression during tacrolimus therapy. *Br J Clin Pharmacol*. 2017;83:2494–2502.
66. Duffy D, Rouilly V, Braudeau C, et al. Standardized whole blood stimulation improves immunomonitoring of induced immune responses in multi-center study. *Clin Immunol*. 2017;183:325–335.
67. Duffy D, Nemes E, Llibre A, et al. Immune profiling enables stratification of patients with active tuberculosis disease or mycobacterium tuberculosis infection. *Clin Infect Dis*. 2021;73(9):e3398–e3408.
68. Drabe CH, Sørensen SS, Rasmussen A, et al. Immune function as predictor of infectious complications and clinical outcome in patients undergoing solid organ transplantation (the ImmuneMo:SOT study): a prospective non-interventional observational trial. *BMC Infect Dis*. 2019;19:573.
69. Mellgren K, Nierop AFM, Abrahamsson J. Use of multivariate immune reconstitution patterns to describe immune reconstitution after allogeneic

stem cell transplantation in children. *Biol Blood Marrow Transplant*. 2019;25:2045–2053.
70. Weinberg K, Blazar BR, Wagner JE, et al. Factors affecting thymic function after allogeneic hematopoietic stem cell transplantation. *Blood*. 2001;97:1458–1466.
71. Annaloro C, Serpenti F, Saporiti G, et al. Viral infections in HSCT: detection, monitoring, clinical management, and immunologic implications. *Front Immunol*. 2020;11: 569381.
72. Nicoli F, Clave E, Wanke K, et al. Primary immune responses are negatively impacted by persistent herpesvirus infections in older people: results from an observational study on healthy subjects and a vaccination trial on subjects aged more than 70 years old. *eBioMedicine*. 2022;76: 103852.
73. Ren M, Guo Q, Guo L, et al. Polymerization of MIP-1 chemokine (CCL3 and CCL4) and clearance of MIP-1 by insulin-degrading enzyme. *EMBO J*. 2010;29:3952–3966.
74. Castellino F, Huang AY, Altan-Bonnet G, et al. Chemokines enhance immunity by guiding naive CD8+ T cells to sites of CD4+ T cell–dendritic cell interaction. *Nature*. 2006;440:890–895.
75. Jabs WJ, Wagner HJ, Maurmann S, Hennig H, Kreft B. Inhibition of macrophage inflammatory protein–1α production by Epstein-Barr virus. *Blood*. 2002;99:1512–1516.
76. Moss P, Rickinson A. Cellular immunotherapy for viral infection after HSC transplantation. *Nat Rev Immunol*. 2005;5:9–20.
77. Basso S, Compagno F, Zelini P, et al. Harnessing T cells to control infections after allogeneic hematopoietic stem cell transplantation. *Front Immunol*. 2020;11: 567531.
78. Ljungman P. Prevention and treatment of viral infections in stem cell transplant recipients. *Br J Haematol*. 2002;118:44–57.
79. Naik S, Vasileiou S, Aguayo-Hiraldo P, et al. Toward functional immune monitoring in allogeneic stem cell transplant recipients. *Biol Blood Marrow Transplant*. 2020;26:911–919.